

# RSC Advances



This is an *Accepted Manuscript*, which has been through the Royal Society of Chemistry peer review process and has been accepted for publication.

*Accepted Manuscripts* are published online shortly after acceptance, before technical editing, formatting and proof reading. Using this free service, authors can make their results available to the community, in citable form, before we publish the edited article. This *Accepted Manuscript* will be replaced by the edited, formatted and paginated article as soon as this is available.

You can find more information about *Accepted Manuscripts* in the [Information for Authors](#).

Please note that technical editing may introduce minor changes to the text and/or graphics, which may alter content. The journal's standard [Terms & Conditions](#) and the [Ethical guidelines](#) still apply. In no event shall the Royal Society of Chemistry be held responsible for any errors or omissions in this *Accepted Manuscript* or any consequences arising from the use of any information it contains.

# Hydrogen Production via Silica Membrane Reactor during Methanol Steam Reforming Process: Experimental Study

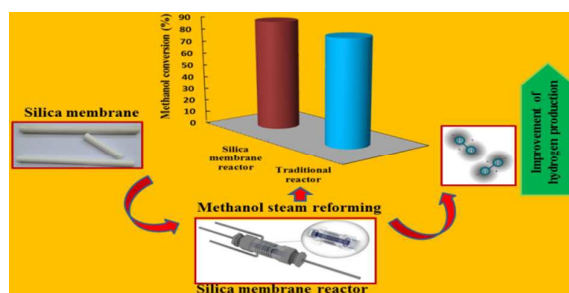
Kamran Ghasemzadeh<sup>1</sup>, Abbas Aghaeinejad-Meybodi<sup>1</sup>, Mohammad Javad Vaezi<sup>1</sup>, Ahmad Gholizadeh<sup>1</sup>, Mohammad Adel Abdi<sup>1</sup>, Ali Akbar Babaluo<sup>\*1</sup>, Mohammad Haghghi<sup>2</sup>, Angelo Basile<sup>3</sup>

<sup>1</sup>Nanostructure Material Research Center (NMRC), Chemical Engineering Department, Sahand University of Technology, Tabriz, Iran.

<sup>2</sup>Reactor and Catalysis Research Center (RCRC), Chemical Engineering Department, Sahand University of Technology, Tabriz, Iran.

<sup>3</sup>ITM-CNR,c/o University of Calabria, Via Pietro Bucci, Cubo 17/C, 87036 Rende (CS), Italy.

## Table of contents



As a first approach, this study presents a comprehensive experimental study of methanol steam reforming for hydrogen production using a tubular silica membrane reactor, in which the modified silica membrane was applied.

\*Corresponding author: a.babaluo@sut.ac.ir  
Tel.: +98 41 3345 9081; fax: +98 41 3344 4355

**Abstract:**

The main purpose of this work is a presentation of experimental operating analysis of silica membrane reactor (MR) for hydrogen production during the methanol steam reforming (MSR) reaction. To implement this performance analysis, a microporous silica membrane is synthesized by polymeric sol gel method. To achieve a high quality of silica membrane, a new strategy is used for surface modification of ceramic support, in which a particles size control of boehmite sol is applied. After evaluation of modified alumina supports, the synthesized silica membrane is characterized and its performance is investigated. The performance analysis of silica membrane in hydrogen purification shows that the H<sub>2</sub>/N<sub>2</sub>, H<sub>2</sub>/CO<sub>2</sub> and H<sub>2</sub>/Ar permselectivity increase sufficiently to 26.18, 22.13 and 29.42, at 200 °C, respectively, so that hydrogen permeance is measured around  $1.1 \times 10^{-6}$  mol.m<sup>-2</sup>.s.Pa at the corresponding conditions. These promising results indicate a high quality of silica membrane for hydrogen production in comparison with the literatures data. To achieve initial purpose of this study, the synthesized silica membrane performance is investigated in MR set up during MSR reaction for hydrogen production. In this case, silica MR performance is compared with traditional reactor (TR) in terms of the methanol conversion, hydrogen yield, hydrogen recovery and CO selectivity. The effects of several operating parameters are also investigated on silica MR performance. In general, the silica membrane presents higher performance with respect to the TR in all ranges of operating parameters. As a specific consequence, a 6% performance enhancement can be obtained by silica MR in compared to TR system.

**Key words:** Hydrogen production, Silica membrane, Membrane reactor, Methanol steam reforming.

## 1. Introduction

During the recent years, there has been a growing interest on developing technologies considering benefit of clean energy sources. The reduction of atmospheric pollution, namely, the emission of greenhouse gases have become imperative and, among the new technologies for mitigating these emissions, fuel cells have the ability to convert chemical into electrical energy efficiently. In particular, the Proton exchange membrane fuel cells (PEMFCs) are zero-pollutants emission systems since they transform the chemical energy of the electrochemical reaction within hydrogen and oxygen into clean electrical power<sup>1,2</sup>.

On the other hand, it should be noted that the high purity hydrogen applications are not restricted to the PEMFCs. Indeed, large quantities of hydrogen are required in the petroleum and chemical industries, so that the most applications of hydrogen are for the processing ("upgrading") of fossil fuels and for the production of ammonia. The major consumers of hydrogen in the petrochemical plant include hydrodealkylation, hydrodesulfurization, and hydrocracking processes.

The hydrogen is industrially produced as a hydrogen-rich stream mainly via steam reforming of natural gas in TRs<sup>3</sup>. In sequence, hydrogen is purified to reach the desired purity for various applications. Indeed, the stream coming out from the TRs commonly contains hydrogen, CO<sub>2</sub>, CO, CH<sub>4</sub> and other byproducts. As a consequence, hydrogen consumers such as PEMFCs supply imposes the purification processes of hydrogen<sup>3,4</sup>. On the other hand, conventional stages of hydrogen purification influence negatively the overall process in terms of costs and efficiency<sup>3</sup>. Hence, scientific attentions have increased to the development of alternative technologies to produce high purity hydrogen. Among them, the MR technology plays an important role as an alternative solution to the conventional systems (TRs + further stages of hydrogen purification) in terms of combination in a single stage of the reforming reaction for hydrogen production and its purification without demanding any further

process/treatment<sup>5</sup>. As shown in Fig. 1, the interest towards this technology is testified by the growing number of scientific publications in the specialized literatures.

### Fig.1

As a particular aspect regarding membrane technology, the inorganic MRs utilization makes possible several advantages over the TRs<sup>3,6-8</sup>. Concerning the membrane kind to be housed in a MR, both MR cost and performance need to be considered. Specifically, several studies have focused on the Pd-based MRs application<sup>9-13</sup>. The Pd-based membranes are highly selective to hydrogen permeation and allow obtaining a high purity hydrogen stream. However, these membranes suffer from cracking during thermal cycling and readily evidence surface contamination by sulfur or carbon monoxide species<sup>14</sup>. Moreover, Pd-based membranes are very expensive and their applications are limited owing to low hydrogen permeability<sup>15,16</sup>. Therefore, an alternative and cheaper solution is strongly needed. On this way, microporous silica membranes are cheaper and present higher permeance, but, on the contrary, they show lower selectivity to hydrogen permeation compared to Pd-based membranes<sup>17-19</sup>.

On the other hand, in terms of processing temperature and CO content, with respect to other feed sources, methanol utilization shows various advantages as a hydrogen carrier for fuel cell applications and, namely, it can be produced from renewable sources<sup>6</sup>. In the meanwhile, the methanol reforming reaction occurs at relatively low temperatures of 240–300 °C, compared to the methane reforming reaction normally performs at 800–1000 °C. Therefore, MSR reaction has been seen as a very attractive and promising process for hydrogen production and, according to the scientific literatures on the argument.

Nevertheless, using silica MRs for carrying out MSR reaction has not been extensively studied. Indeed, to our best knowledge, a few studies have been presented for silica MR performance in MSR reaction<sup>20-26</sup>. According to our pervious modeling works<sup>23-26</sup>, the

promising results have justified a necessity for comprehensive experimental study of the potential advantages achievable by using a silica MR.

Therefore, the present work aims to evaluate and compare the performance attainable in silica MR by carrying out MSR reaction. Moreover, a comparison with a TR, working at the same operating conditions of MR, was realized. To perform this study, as a first approach, a silica membrane is synthesized with high hydrogen permeance on the modified  $\gamma$ - alumina support, in which support surface is modified using a new strategy of size distribution control of sol particles. After analyzing the synthesized silica membrane efficiency for hydrogen purification, the silica membrane performance in the MR set up is investigated for MSR process. A set of experimental results are then provided which illustrate some key points about the silica MR performance in terms of the methanol conversion, hydrogen recovery, total hydrogen yield and CO selectivity versus some important operating parameters such as reaction temperature, feed molar ratio and gas hourly space velocity (GHSV).

## **2. Experimental**

### **2.1. Materials**

In this experimental study, the material sources were used as follow: Tetraethylorthosilicate (TEOS, 98%, Sigma Aldrich) as silicon source, Nitric acid ( $\text{HNO}_3$ , 65%, Merck) as catalyst for silica sol preparation, Ethanol ( $\text{EtOH}$ , 99.9% Merck) as solvent, Methanol ( $\text{MeOH}$ , 99.9% Merck) and deionized water as feed for steam reforming and Polyethylene glycol (PEG, Merck, Molecular weight: 35000) as stabilizer for Boehmite sol preparation and also, Aluminum -tri-sec-butylate (ATSB, 97%, Merck) as source of  $\gamma$ -alumina.

### **2.2. Surface modification of ceramic support**

#### **2.2.1. Support preparation**

According to the author's pervious works<sup>27</sup>, the homemade supports applied for membrane synthesis were  $\alpha$ -alumina tubes with thickness of 4 mm, diameter of 11 mm, length of 70

mm, average pore size of ~ 570 nm and average porosity of 47.2%. Before the  $\gamma$ -alumina synthesis, the supports were cleaned in deionized water by ultrasonic regenerator for 10 min and then dried at 40 °C for 12 h.

### 2.2.2. Support modification

In order to modify the pore structure of porous  $\alpha$ -alumina substrates, the boehmite sol as material for intermediate layers were prepared. The boehmite sol was prepared by method of Uhlhorn et al.<sup>28</sup>, although, an innovation was applied for sol preparation in this study. In this procedure, the boehmite sol preparation was carried out by adding ATSB dropwise to deionized water, in which about 1.5 L of water was added per mole alkoxide at 80 °C and under vigorous stirring. Then, a white solution was obtained, which was peptized with nitric acid. The resulting colloidal suspension was kept boiling until the most of the butanol to be evaporated. The PEG solution was made by dissolving PEG (1wt% of sol) in deionized water under vigorous stirring and then was added to sol. It should be noted that the nitric acid was added to decrease the range of pH till 3-4 and after spending 1 h time in this step, sol was refluxed for 16 h to form a stable boehmite sol.

The dip coating process was performed at room temperature, in which the substrate speed and dip-time were  $1\text{mm}\cdot\text{s}^{-1}$  and 10 s, respectively. After dipping step, the membranes were dried at 40 °C at least for 24 h. Subsequently, the  $\gamma$ -alumina layer was formed by calcining at 650 °C for 3 h in atmospheric condition with a heating and cooling rate of 0.5 °C/min. The whole processes of dipping, drying and calcining were repeated 4 times. As first approach, the particle size distribution of boehmite sol was altered for each step of coating. Varying the particle size distribution of sol was provided by changing nitric acid and aging time. In fact, aging time means the period time before adding the nitric acid to boehmite sol. The

conditions of boehmite sol preparation for different intermediate modified layers are presented in Table 1.

**Table 1.**

### **2.3. Silica membrane preparation**

The microporous silica membrane top-layer was prepared by dipping the modified  $\gamma$ -alumina mesoporous substrate in the silica standard solution, and followed by calcining. In this method, a mixture of acid and water is carefully added to a mixture of TEOS and ethanol under vigorous stirring, while during the addition of the acid/water mixture, the TEOS/ethanol mixture is placed in an ice-bath to avoid partial hydrolysis<sup>29</sup>. Then, the reaction mixture was refluxed for 3 h at 60 °C in the oil bath under uniform stirring. The reaction mixture had a final molar TEOS/ethanol/water/acid ratio of 1/3.8/6.4/0.085. The reacted mixture was cooled and diluted 19 times with ethanol to obtain the final dip solution. The modified  $\gamma$ -alumina substrate was coated by prepared silica solution, so that the coating speed was  $1\text{mm}\cdot\text{s}^{-1}$  and the dip-time was 10 s. After dipping step, the membrane was calcined at 600 °C for 3 h at atmospheric condition with a heating and cooling rate of 1 °C/min. The whole processes of dipping and calcining were repeated 5 times to eliminate the defects in the silica membrane layer structure.

### **2.4. Characterization and permeance tests**

The meso/microstructure and morphology of the synthesized membrane were studied by scanning electron microscope (SEM) and Energy dispersive X-ray spectrometer (EDAX, Phoenix) measurements.

The permeation tests were carried out using custom-made stainless steel module, designed for 70 mm tubular membranes. A schematic of permeation set up is shown in Fig.S1, in which gases permeation was measured based on constant pressure method.

The membrane ends were sealed in the module using Witon and Teflon bronze O-rings, which allow measuring at high temperatures (up to 300 °C). For modified  $\gamma$ -alumina mesoporous membrane, only pure gas permeance ( $H_2$  and  $N_2$ ) tests were performed at ambient temperature, while for silica membrane, pure gases ( $H_2$ ,  $N_2$ ,  $CO_2$  and Ar) tests were carried out at different temperatures (25, 100, 200 and 300 °C). Moreover, all the permeance tests were investigated at different gradient pressure (1, 2, 3 and 4 bar) and the permselectivity ( $F_\alpha$ ) was obtained by the ratio of single gases permeances.

## 2.5 Silica MR tests

In this case, the silica MR performance was compared with TR. Fig. 2 shows a schematic of the experimental set up used for MSR reaction.

**Fig. 2.**

The experimental setup of the MR consists of tubular stainless steel module (Length 260 mm, I.D. 24 mm) housing and a tubular microporous silica membrane that is selective to hydrogen (O.D. 11 mm, total length 70 mm and active length 50 mm) which was produced during this study. As shown in Fig. 3, two zones can be identified into the MR: a first zone, inside the membrane (lumen side), where permeate flow (mostly hydrogen) is collected and a second one corresponding to the annulus of the MR (shell side), where the reaction is take placed.

Regarding to the flow hydrodynamic in TR, the silica membrane was replaced with a metal profile tube.

A schematic of silica membrane module is illustrated in Fig. 3. For the silica MR and TR in MSR reaction, 1 g of commercial Cu/ZnO/Al<sub>2</sub>O<sub>3</sub> catalyst (ICI 83-3, furnished by Syntex), was filled into the shell side and glass spheres (1 mm diameter) mixed and also were placed into both end sides of module to prevent the motion of the catalyst due to the gas flow. Two Teflon-bronze O-rings ensure that permeate and retentate streams don't mix with each other in the module at high temperatures.

Before the reaction, the catalyst was pretreated for 3 h with hydrogen and nitrogen flow ( $1.1 \times 10^{-2}$  mol.min<sup>-1</sup>), at an atmospheric pressure and temperature of 320 °C to reduce copper oxide to metal Cu. A flat temperature profile along the furnace was confirmed during the reaction by means of a three points thermocouple placed into the furnace.

**Fig. 3.**

During the MSR process, the H<sub>2</sub>O/MeOH mixture was evaporated in a preheating line, and diluted by argon carrier gas, in which argon carrier gas was used with flow rate of 25 mL/min. The concentration of products and reactants in the retentate and permeate side was analyzed using gas chromatography equipped with a packed porapak Q column. Each experimental point obtained in this work represents an average value of 7 experimental points taken in 180 min at steady-state conditions.

The following definitions were used for describing the silica MR/TR performances:

$$\text{Methanol - Conversion(\%)} = \frac{\text{CH}_3\text{OH}_{\text{out}} - \text{CH}_3\text{OH}_{\text{in}}}{\text{CH}_3\text{OH}_{\text{in}}} \times 100 \quad (4)$$

where CH<sub>3</sub>OH<sub>in</sub> is the methanol molar feed flow rate and CH<sub>3</sub>OH<sub>out</sub> is the methanol flow rate in the MR outlet.

$$\text{Total hydrogen yield (\%)} = \frac{(H_{2\text{-permeate}} + H_{2\text{-retentate}})}{3.CH_3OH_{\text{in}}} \times 100 \quad (5)$$

$$\text{Hydrogen recovery (\%)} = \frac{H_{2\text{-permeate}}}{H_{2\text{-permeate}} + H_{2\text{-retentate}}} \times 100 \quad (6)$$

$$\text{Selectivity (\%)} = \frac{X_{\text{out}}}{H_{2\text{-out}} + CO_{\text{out}} + CO_{2\text{-out}}} \quad (7)$$

where  $H_{2\text{-permeate}}$  is the hydrogen molar flow rate that permeates through the silica membrane,  $H_{2\text{-retentate}}$  is the hydrogen molar flow rate in retentate side and X can be  $H_2$ ,  $CO_2$ , CO. Among the mentioned definitions, Eq. 6 was only related to the MR.

### 3. Result and discussion

#### 3.1. Modified membrane support

In the preparation of nanostructure silica membranes, the quality of the support is very effective on the membrane layer integrity. The surface roughness and homogeneity of the support determine not only the integrity of the selective silica layer but also the minimal thickness of the silica layer for complete surface coverage<sup>30, 31</sup>. The use of thin intermediate layers is an attractive alternative which can be used to generate a smooth surface, to improve the chemical adhesion of the silica layer to the support, to limit the effect of differential thermal expansion coefficients, and finally, to limit the diffusion of the silica sol in the support pores.

According to literature<sup>32</sup>, the  $\gamma$ -alumina layer is mostly used as an intermediate membrane layer for the development of a gas separation membrane. These layers are not susceptible to crack-formation and peeling-off effects during the firing process. Hence, to modify the homemade  $\alpha$ -alumina tubular supports, the  $\gamma$ -alumina layer was prepared as intermediate layer in synthesizing the nanostructure silica membrane. However, in order to improve the surface modification of ceramic support, a new technique for synthesis of the intermediate  $\gamma$ -

alumina layers was suggested, so that size distribution control of sol particles in each step of coating was applied.

Fig. 5 shows the SEM micrographs of the surface and the cross-section of  $\gamma$ -alumina/ $\alpha$ -alumina support. Pore size and surface roughness of the  $\alpha$ -alumina support were clearly reduced, in which the pore sizes of such  $\gamma$ -alumina layers are recognized to be in the 3–5 nm range. Moreover, after 4 times coating, as shown in Fig.5, the thickness of  $\gamma$ -alumina layer is around 10  $\mu\text{m}$ .

**Fig. 4.**

Furthermore, the gas permeation tests were conducted to observe the effect of modification using the  $\gamma$ -alumina layers. As presented in Fig. S2, the slope of  $\text{N}_2$  and  $\text{H}_2$  permeances were decreased after modifying the support with respect to the unmodified support. On the other hand, pressure dependence of gas permeance was decreased. This result indicated that the gas permeance mechanism was approximately changed from viscose flow to Knudsen diffusion.

As reported in Table S1, the permselectivity of  $\text{H}_2/\text{N}_2$  (higher than 3.2, and relatively near to Knudsen diffusion mechanism (3.74)) absolutely validates formation of mesoporous layer on  $\alpha$ -alumina support. The  $\text{H}_2/\text{N}_2$  permselectivity is decreased by increasing the pressure difference and this trend is probably related to more effects of macropores or micro-defects on permeance at high pressure differences.

Corresponding to the obtained results, a suitable uniformity and roughness of  $\gamma$ -alumina membrane was achieved by using control of particle size distribution in boehmite sol preparation in comparison with the literature<sup>31</sup>.

### 3.2. Silica membrane

According to high stability and quality of the modified  $\gamma$ -alumina support, the silica membrane was synthesized on the modified support via sol-gel method. The SEM observation results of silica membrane surface and cross section are shown in Fig.5.

As depicted, the  $\alpha$ -alumina support,  $\gamma$ -alumina layer and silica membrane layer are approximately recognized and the homogenous crack-free silica layer was formed.

However, the SEM image does not clearly distinguish the top layer from the  $\gamma$ -alumina intermediate layer or  $\alpha$ -alumina substrate. Therefore, an EDAX analysis was also carried out for investigating the quality of synthesized silica membrane. As EDAX analysis was depicted in Fig.S3, formation of silica layer on modified  $\gamma$ -alumina is confirmed, so that diffusion of the silica particles into the support is negligible.

**Fig.5.**

The activated transport or molecular sieving mechanism as reported in the literature<sup>31</sup> has a temperature dependency flux as follow:

$$J = J_0 \cdot \exp\left(\frac{-E_a}{RT}\right) \frac{dp}{dl}$$

(8)

$J_0$  is a temperature independent coefficient and  $E_a$  is the apparent activation energy.  $E_a$  is the sum of two contributions: the heat of sorption of the molecule that is a negative number, because adsorption is an exothermic process and the positive activation energy of mobility of the permeating molecule inside the membrane matrix. Since these two terms have opposite signs, the apparent activation energy can be positive or negative depending on their relative magnitudes<sup>33</sup>.

Fig. 6 shows the observed pure gas ( $H_2$ ,  $CO_2$  and Ar) permeance versus increasing pressure difference for the synthesized silica membrane at different temperatures of 25, 100 and 200

°C. By referring to the obtained results, increasing the gas permeance by pressure difference due to the enhancement of driving force is reasonable.

**Fig.6.**

According to dual trend of gas permeance versus temperature, as depicted in Figs. 6 and S4, the permeance of H<sub>2</sub> through the silica membrane is activated and increased with temperature. Therefore, regarding to Fig. S4 and Eq. 9, the activation energy of H<sub>2</sub> permeation in synthesized silica membrane is calculated positive value around 10.1 kJ/mol and consequently the molecules have larger adsorption on the silica surface at higher temperatures, while the permeation of CO<sub>2</sub> and Ar are decreased with temperature. Hence, the activation energies of CO<sub>2</sub> and Ar are achieved the negative values equal to -3.1 and -1.9 kJ/mol, respectively.

Moreover, as reported in Table 2, the permselectivity of H<sub>2</sub>/CO<sub>2</sub>, H<sub>2</sub>/N<sub>2</sub> and H<sub>2</sub>/Ar remarkably increased by enhancement of the temperature due to higher H<sub>2</sub> permeance and lower CO<sub>2</sub>, N<sub>2</sub> and Ar permeances at higher temperatures. This result is another confirmation of activated transport mechanism in the synthesized silica membrane.

**Table 2.**

A direct comparison among all the experimental data from literatures reported in Table 3 is not possible owing to the different operating conditions adopted by each author. Nevertheless, from a qualitative point of view it is possible to observe that most of the H<sub>2</sub>/N<sub>2</sub> and H<sub>2</sub>/CO<sub>2</sub> permselectivity values for silica membrane from the literatures are concentrated between 100 and 500 °C. Hence, it is found that the permselectivity values are increased by enhancement of temperature and pressure difference.

This aspect visualizes to the reader a scenario in which great performance is achievable by the synthesized silica membrane. According to the use of a similar sol gel method for

synthesizing of silica layer, the higher performance of silica membrane probably is related to good surface modification of  $\alpha$ -alumina support by  $\gamma$ -alumina intermediate layers.

**Table 3.**

### **3.3. Silica MR performance in MSR process**

To understand the ability of synthesized silica membrane, an experimental study has been carried out for evaluating the effect of most important operating conditions on silica MR performance compared to TR, in terms of methanol conversion, total hydrogen yield, CO selectivity and hydrogen recovery. In particular, the effect of feed molar ratio, reaction temperature and gas hour space velocity (GHSV) was investigated for both of the silica MR and TR.

Table 4 reports the operating conditions used for carrying out MSR reaction in both silica MR and TR. In general, the experimental analysis can be divided into three parts, in which feed molar ratio, reaction temperature and GHSV are changed.

**Table 4.**

#### **3.3.1. Evaluation of reaction temperature effect**

The influence of temperature on both silica MR and TR performances in terms of methanol conversion (Eq.5), total hydrogen yield (Eq.6), hydrogen recovery (Eq.7) and CO selectivity (Eq.8) was evaluated. As reported in Table 6, the experiments were carried out by maintaining the reaction pressure equal to 1.5 bar,  $H_2O/CH_3OH = 3$  and  $GHSV = 6000 h^{-1}$ . The reaction temperature has been varied between 240 and 300 °C.

Fig. 7 shows methanol conversion versus reaction temperature for two cases, namely silica MR and TR. For each case, methanol conversion increases with rising the temperature owing

to the endothermic character of the reaction system. Moreover, it is evident that higher methanol conversion is achievable by using silica MR with respect to TR due to the products removal from reaction zone through the silica membrane, which shifts the reactions towards a further products formation with consequent methanol consumption.

Furthermore, Fig. 8 shows total hydrogen yield versus reaction temperature for both silica MR and TR. The hydrogen yield is improved by increasing the reaction temperature in both cases. In fact, by considering the Eq.6, a higher temperature can result in a higher hydrogen production rate during MSR reaction. On the other hand, it is clear that higher hydrogen yield is achievable by using silica MR with respect to TR owing to the products removal from reaction zone through the silica membrane which can shift the MSR reaction towards a further hydrogen formation.

**Fig.7.**

**Fig.8.**

A further comparison between the silica MR and TR is presented in Table 5, where the CO selectivity values are reported as function of the reaction temperature.

**Table 5.**

This table shows the lower CO selectivity in the silica MR with respect to the TR outlet composition at feed molar ratio of 3, GHSV equal to  $6000 \text{ h}^{-1}$  and reaction pressure of 1.5 bar. This result can be ascribed to the "shift effect", which induced the shift of the WGS reaction towards the products, allowing a greater CO consumption in the silica MR.

Moreover, it's evident that CO selectivity is increased by enhancement of reaction temperature for both cases. It can be related to more role of methanol decomposition (MD) reaction in higher temperature.

Meanwhile, as reported in Table 5, the hydrogen recovery is improved by increasing the reaction temperature in silica MR. In fact, by regarding to the Eq. 7, a higher temperature results in a higher hydrogen permeation flux involving a higher hydrogen stream recovered in the permeate side. However, it should be noted that lower values of hydrogen recovery can be improved by increasing reaction pressure<sup>23-26</sup>.

### 3.3.2. Evaluation of feed molar ratio effect

Another important operating parameter taken into account in present study is the feed molar ratio (Steam/ MeOH). The influence of feed molar ratio on the both silica MR and TR performances in terms of methanol conversion and hydrogen recovery was evaluated. According to MSR reaction, an enhancement of steam/MeOH can shift the reaction toward the products. Therefore, regarding to the Chatelier's principle, methanol conversion and hydrogen production can be improved by increasing the feed molar ratio.

As reported in Table 4, the experimental tests were carried out at 300 °C, 1.5 bar and GHSV = 6000 h<sup>-1</sup> by varying the steam/MeOH between 1 and 3.

Fig. 9 shows that the methanol conversion is increased by enhancement of feed molar ratio. In particular, at feed molar ratio of 3, the methanol conversion was achieved 88.7% for silica MR, where 84.4 % methanol conversion obtained for TR. It is clear that higher performance grade of silica MR with respect to TR in feed molar ratio of 3 is lower than once can be achieved in feed molar ratio of 1. This phenomenon is probably related to steam concentration polarization effect on the silica membrane.

Moreover, as depicted in Fig. 10, increasing the feed molar ratio from 1 up to 3 can increase hydrogen production and, as consequence, total hydrogen yield. It's obvious that higher total hydrogen yield is achievable by using silica MR with respect to TR owing to the shift effect. By comparing the Figs.9 and 10, the similar trend of methanol conversion was obtained for

hydrogen yield at higher feed molar ratio with respect to lower molar ratio. It means that the higher steam value can effect on silica performance, nevertheless, performance loss is only 3% for higher feed molar ratio (Steam/MeOH=3).

**Fig.9.**

**Fig.10.**

Another comparison terms between the silica MR and TR are shown in Table 6, where the CO selectivity values and hydrogen recovery are reported as function of feed molar ratio.

**Table 6.**

Table 8 indicates the lower CO selectivity in the silica MR with respect to the TR outlet composition at reaction temperature of 300 °C, GHSV equal to 6000 h<sup>-1</sup> and reaction pressure of 1.5 bar. This result can be referred to the "shift effect" induced the shift of the WGS reaction towards the products (CO<sub>2</sub> and H<sub>2</sub>) and allowed a greater CO consumption in the silica MR. In addition, the CO selectivity is decreased by increasing the steam ratio in both cases of silica MR and TR.

Furthermore, as illustrated in Table 6, the hydrogen recovery is decreased by enhancement of feed molar ratio. The trend observed in this table is probably due to steam concentration polarization effect on the silica membrane and consequently the lower hydrogen permeation inside the silica MR at high feed molar ratios.

### **3.3.3. Evaluation of GHSV effect**

A further parameter that can strongly affect the silica MR and TR performance is the GHSV. In this case, the experiments were accomplished at 300 °C, 1.5 bar and steam/MeOH=3 by

varying the GHSV between  $6000 \text{ h}^{-1}$  and  $10000 \text{ h}^{-1}$ . As reported in Table 7, the methanol conversion is decreased by increasing the GHSV for the silica MR and TR. By decreasing the GHSV, a higher residence or contact time in reaction zone is favored. In fact, the lower values of GHSV can favour to hydrogen formation in reaction side. Therefore, a greater methanol conversion and hydrogen yield can be justified by decreasing the GHSV. Indeed, this effect produces a higher retentate hydrogen partial pressure that enhances the hydrogen permeation driving forces with a consequent more effective shifting of the MSR reaction towards the products. Therefore, this gives more methanol consumption and a greater hydrogen production as well as a higher hydrogen stream permeating through the membrane. Hence, the higher performance of silica MR with respect to TR in terms of methanol conversion and hydrogen yield can be realized (see Table 7).

**Table 7.**

Table 8 specifies the trend of CO selectivity and hydrogen recovery versus GHSV values. It is found that hydrogen recovery is improved by decreasing GHSV. In fact, higher retentate hydrogen partial pressure due to higher hydrogen production rate in lower GHSV values is the main specification of hydrogen recovery improvement.

**Table 8.**

Moreover, the CO selectivity is decreased by enhancement of GHSV. Indeed, this trend can conclude a lower conversion of WGS reaction in the higher GHSV values. On the other hand, the lower CO values in silica MR with respect to TR can be referred to the extractor role of hydrogen through the silica membrane.

A further investigation was carried out for analyzing the molar compositions during MSR reaction for silica MR with respect to TR. As reported in Table S2, regarding to feed and permeate flow rates, it can be concluded a higher hydrogen and lower carbon monoxide flow rates in the silica MR in compared to the TR.

#### 4. Conclusion

In present work, high quality microporous silica membrane was synthesized by polymeric sol gel method showing a temperature dependency flux of activated transport. In synthesis of composite silica membrane, a new successful strategy was used for surface modification of  $\alpha$ -alumina support, in which a particles size control of boehmite sol was applied. The permeance test results strongly suggest that the higher quality of surface modification of supports can affect directly the silica membrane performance. Hence, the improvement of silica membrane performance can extend its application. Regarding to main purpose of work, the analysis of the methanol conversion, hydrogen yield, hydrogen recovery and CO selectivity was performed in silica MR during MSR reaction. According to results, it was concluded that methanol conversion and total hydrogen yield improved by increasing the reaction temperature and feed molar ratio and also by decreasing the GHSV, while CO selectivity decreased by variations mentioned above. However, increasing the feed molar ratio had negative effect in term of hydrogen recovery. As a consequence, a 6% enhancement of performance can be achieved by silica MR in comparison with TR. As a future direction, this study indicate that silica MR can be introduced as a promising option for hydrogen production in comparison with competitive processes.

**Acknowledgments**

The Authors wish to thank Sahand University of Technology (SUT) for the financial support of this work. Also, thank co-workers and technical staff in the department of chemical engineering, the ITM-CNR and nanostructure materials research center (NMRC) of SUT for their help during various stages of this work.

**Acronyms list:**

ATSB: Aluminum -tri-sec-Butylate.

Ethanol: EtOH.

GHSV: Gas hourly space velocity.

Methanol: MeOH.

MR: Membrane reactor.

MSR: Methanol steam reforming.

PEMFC: Proton exchange membrane fuel cell.

MD: Methanol decomposition.

SEM: Scanning electronic microscope.

TEOS: Tetraethylorthosilicate.

TR: Traditional reactor.

WGS: Water gas shift.

## References

---

1. J. Wee, *Renew. Sust. Energ. Rev.*, 2007, **11**, 1720.
2. S. Bose, T. Kuila, T. X. H. Nguyen, *Prog. Polym. Sci.*, 2011, **36**, 813.
3. A. Iulianelli, P. Ribeirinha, A. Mendes, A. Basile, *RENEW. SUST. ENERG. REV.*, 2014, **29**, 355.
4. R. Y. Chein, Y. C. Chen, Y. S. Lin, J. N. Chung, *Int. J. Hydrogen. Energ.*, 2012, **36**, 466.
5. G. Q. Lu, J. C. Diniz de Costa, M. Duke, S. Giessler, R. Socolow, R. H. Williams, *J. Colloid. Interface Sci.*, 2007, **314**, 589.
6. S. Xiu, A. Shahbazi, *Int. J. Hydrogen. Energ.*, 2012, **16**, 4406.
7. A. Basile, A. Iulianelli, T. Longo, S. Liguori, M. De Falco, Pd-based selective membrane State of the Art. In: Membrane reactors for hydrogen production processes, L Marrelli, M De Falco & G Iaquaniello, editors, Springer London Dordrecht Heidelberg New York; 2011, ch. 2, pp.21–55.
8. A. S. Damle, *J. Power. Sources.*, 2009, **186**, 167.
9. A. Iulianelli, T. Longo, A. Basile. *J. Membr. Sci.*, 2008, **323**, 235.
10. B. K. R. Nair, M. P. Harold, *Chem. Eng. Sci.*, 2006, **61**, 6616–6636.
11. A. Basile, A. Parmaliana, S. Tosti, A. Iulianelli, F. Gallucci, C. Espro, J. Spooen, *Catal. Today.*, 2008, **13**, 717.
12. F. Gallucci, A. Basile, S. Tosti, A. Iulianelli, E. Drioli, *Int. J. Hydrogen. Energ.*, 2007, **32**, 1201.
13. C. H. Fu, J. C. S. Wu, *Int. J. Hydrogen. Energ.*, 2007, **32**, 4830.
14. L. Shao, B. T. Low, T. S. Chung, A. R. Greenberg, *J. Membr. Sci.*, 2009, **327**, 18.
15. A. F. Ismail, L. I. B. David, *J. Membr. Sci.*, 2001, **193**, 1.
16. G. A. Szejner, I. Efremenko, M. Sheintuch, *AIChE J.*, 2004, **50**, 224.

17. B. N. Nair, W. J. Elferink, K. Keizer, H. Verweij, *J. colloid. Interface Sci.*, 1996, **78**, 565.
18. R. M. de Vos, W. F. Maierb, H. Verweij, *J. Membr Sci.*, 1999, **158**, 277.
19. D.W. Lee, S. J. Park, C. Y. Yu, S. K. Ihm, K. H. Lee, *J. Membr Sci.*, 2007, **302**, 265.
20. A. Jabbari, K. Ghasemzadeh, P. Khajavi, F. Assa, M. A. Abdi, A. A. Babaluo, A. Basile, *Int. J. Hydrogen. Energ.*, 2014, DOI: 10.1016/j.ijhydene.2014.05.056.
21. D. W. Lee, S. J. Park, C. Y. Yu, S. K. Ihm, K. H. Lee, *J. Membr Sci.*, 2008, **316**, 63.
22. D. W. Lee, S. E. Nam, B. Sea, S. K. Ihm, K. H. Lee, *Catal. Today.*, 2006, **118**, 198.
23. K. Ghasemzadeh, P. Morrone, A. A. Babalou, A. Basile, *Int. J. Hydrogen. Energ.*, 2014, DOI: 10.1016/j.ijhydene.2014.04.010.
24. K. Ghasemzadeh, P. Morrone, S. Liguori, A. A. Babalou, A. Basile, *Int. J. Hydrogen. Energ.*, 2013, **38**, 16698.
25. K. Ghasemzadeh, P. Morrone, A. Iulianelli, S. Liguori, A. A. Babalou, A. Basile, *Int. J. Hydrogen. Energ.*, 2013, **38**, 10315.
26. K. Ghasemzadeh, S. Liguori, P. Morrone, A. Iulianelli, V. Piemonte, A. A. Babaluo, A. Basile, *Int. J. Hydrogen. Energ.*, 2013, **38**, 16685.
27. A. A. Babaluo, M. Kokabi, M. Manteghian, R. Sarraf-Mamoory, *J. Eur. Ceram. Soc.*, 2004, **24**, 3779.
28. R. J. R. Uhlhorn, K. Keizer, A. J. Burggraaff, *J. Mater. Sci.*, 1992, **27**, 527.
29. R. M de Vos, H. Verweij, *J. Membr Sci*, 1998, **143**, 37.
30. R. S. A. Lange, K. Keizer, A. J. Burggraaf, *J. Membr Sci.*, 1995, **99**, 57.
31. A. Ayrat, A. Julbe, V. Rouessac, S. Roualdes, J. Durand, *Membr Sci Technol.*, 2008, **13**, 33.
32. T. V. Gestel, D. Sebold, F. Hauler, W. A. Meulenber, H. P. Buchkremer, *J. Membr Sci.*, 2010, **359**, 64.

33. V. Boffa, J. E. ten Elshof, R. Garcia, D. H. A. Blank, *Microporous Mesoporous Mater.*, 2009, **118**, 202.
34. M. Pakizeh, M. R. Omidkhah, A. Zarringhalam, *Int. J. Hydrogen. Energ.*, 2007, **32**, 1825.
35. J. P. Collins, R. W. Schwarts, R. Sehgal, T. L. Ward, C. J. Brinker, G. P. Hagen, C. A. Udovich, *Ind. Eng. Chem. Res.*, 1996, **35**, 4398.
36. R. Bredesen, K. Jordal, O. Bolland, *Chem. Eng. Process.*, 2004, **43**, 1129.

**List of Figures:**

**Fig. 1.** Number of scientific papers on H<sub>2</sub> production by MR technology versus year.

Scopus database: [www.scopus.com](http://www.scopus.com).

**Fig.2.** Schematic of permeation test set up.

**Fig.3.** Schematic flow-sheet of silica MR set up.

**Fig.4.** SEM images of the modified  $\gamma$ -alumina support prepared by control of particles size:

(a) surface and (b) cross-section.

**Fig.5.** SEM images of (a) surface and (b) cross section of silica membrane.

**Fig.6.** Pure gases permeance versus pressure difference at various temperatures: (a) H<sub>2</sub>, (b)

CO<sub>2</sub> and (c) Ar.

**Fig.7.** Methanol conversion versus reaction temperature for the silica MR and TR

(at 1.5 bar, H<sub>2</sub>O/CH<sub>3</sub>OH=3 and GHSV=6000 h<sup>-1</sup>).

**Fig.8.** Total hydrogen yield versus reaction temperature for the silica MR and TR (at 1.5 bar,

H<sub>2</sub>O/CH<sub>3</sub>OH=3 and GHSV=6000 h<sup>-1</sup>).

**Fig.9.** Methanol conversion versus feed molar ratio (steam/MeOH) for the silica MR and TR

(at 1.5 bar, 300 °C and GHSV=6000 h<sup>-1</sup>).

**Fig.10.** Total hydrogen yield versus feed molar ratio (Steam/MeOH) for the silica MR and

TR (at 1.5 bar, 300 °C and GHSV=6000 h<sup>-1</sup>).

**List of Tables:**

**Table 1.** The conditions of boehmite sol preparation and its particle size distribution for different layers.

**Table 2.** H<sub>2</sub>/CO<sub>2</sub>, H<sub>2</sub>/N<sub>2</sub> and H<sub>2</sub>/Ar permselectivity at different temperatures ( $\Delta p=2\text{bar}$ ).

**Table 3.** Comparing performance of synthesized silica membrane in this work with literatures data.

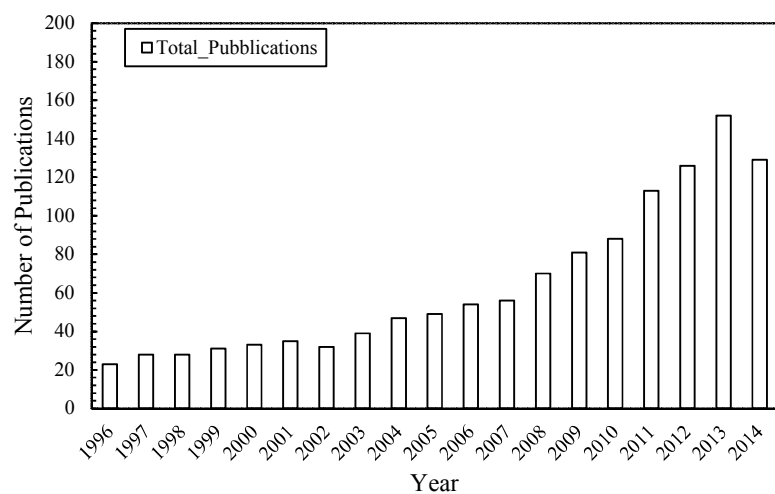
**Table 4.** The investigated conditions for the silica MR and TR.

**Table 5.** CO selectivity and hydrogen recovery for silica MR and TR versus reaction temperature (at Steam/MeOH=3, 1.5 bar and GHSV=6000 h<sup>-1</sup>).

**Table 6.** CO selectivity and hydrogen recovery for silica MR and TR versus feed molar ratio (at 300 °C, 1.5 bar and GHSV=6000 h<sup>-1</sup>).

**Table 7.** Methanol conversion and total hydrogen yield for silica MR and TR versus GHSV (at 300 °C, 1.5 bar and feed molar ratio 3).

**Table 8.** The CO selectivity and hydrogen recovery for silica MR and TR versus GHSV (at 300 °C, 1.5 bar and feed molar ratio 3).

**Figures:**

**Fig. 1.** Number of scientific papers on H<sub>2</sub> production by MR technology versus year.  
Scopus database: [www.scopus.com](http://www.scopus.com).

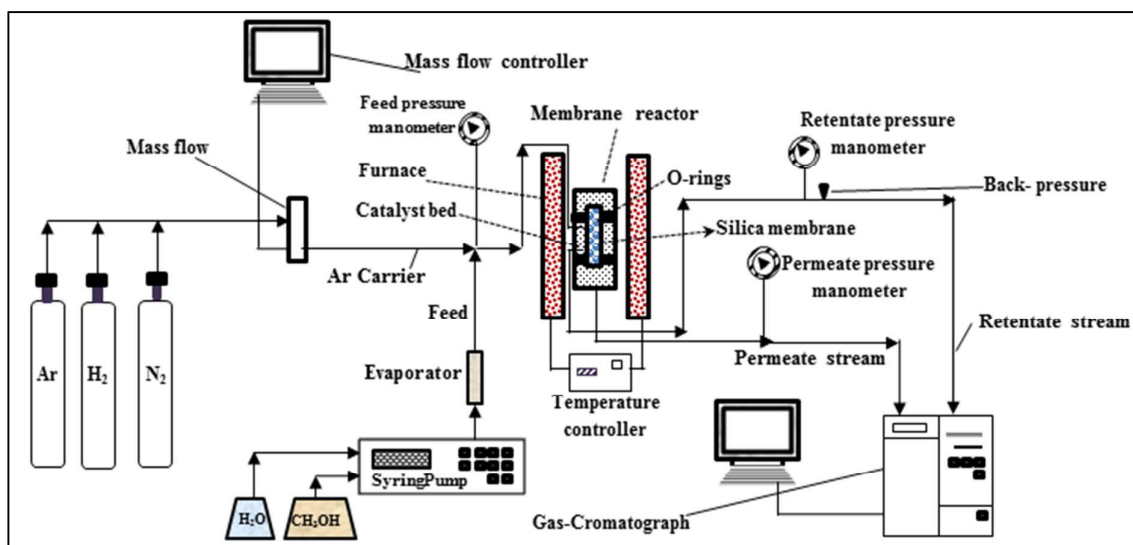
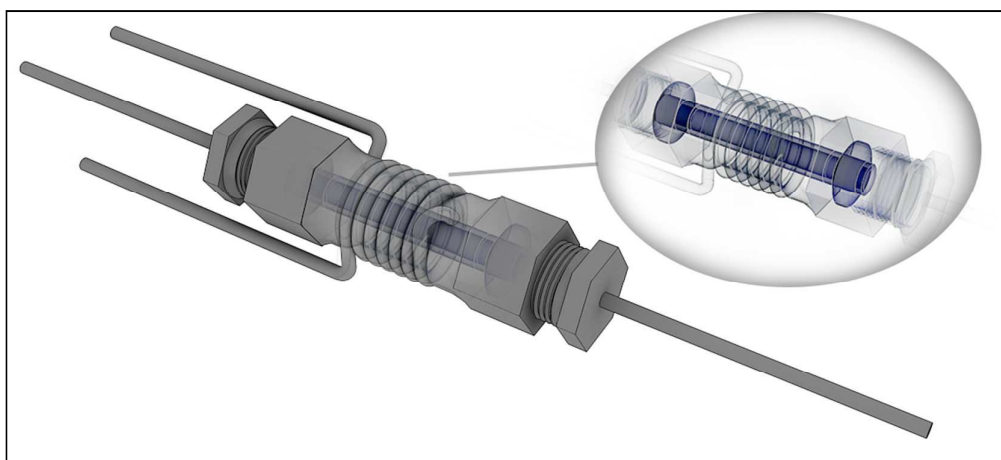
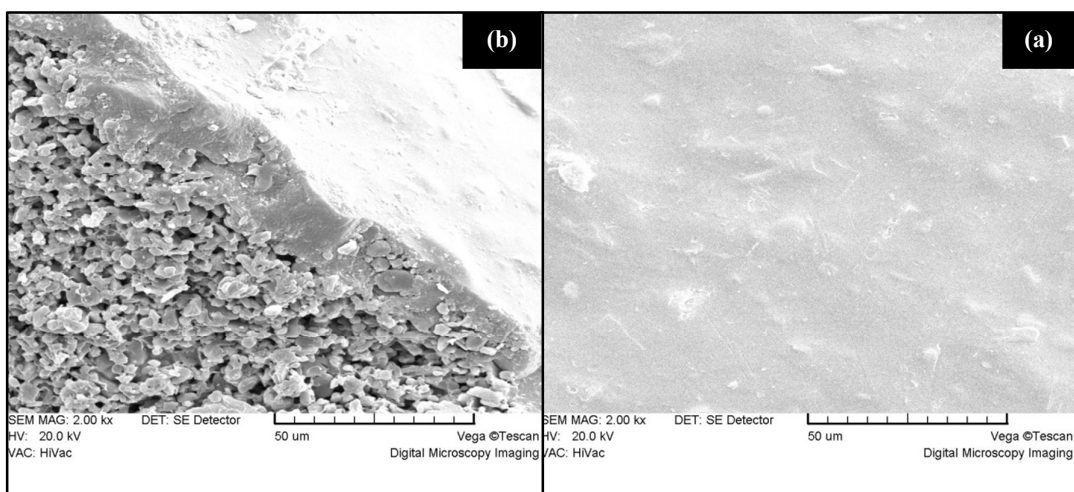


Fig.2: Schematic flow-sheet of silica MR set up.



**Fig. 3:** Schematic of membrane module housing composite silica membrane in MR set up.



**Fig. 4:** SEM images of the modified  $\gamma$ -alumina support prepared by control of particles size: (a) surface and (b) cross-section.

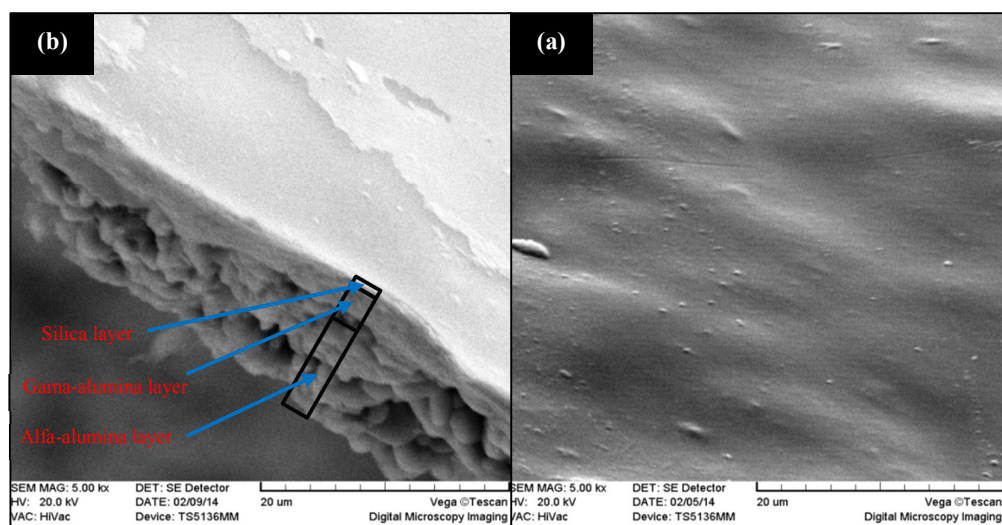


**Fig. 5:** SEM images of (a) surface and (b) cross section of silica membrane.

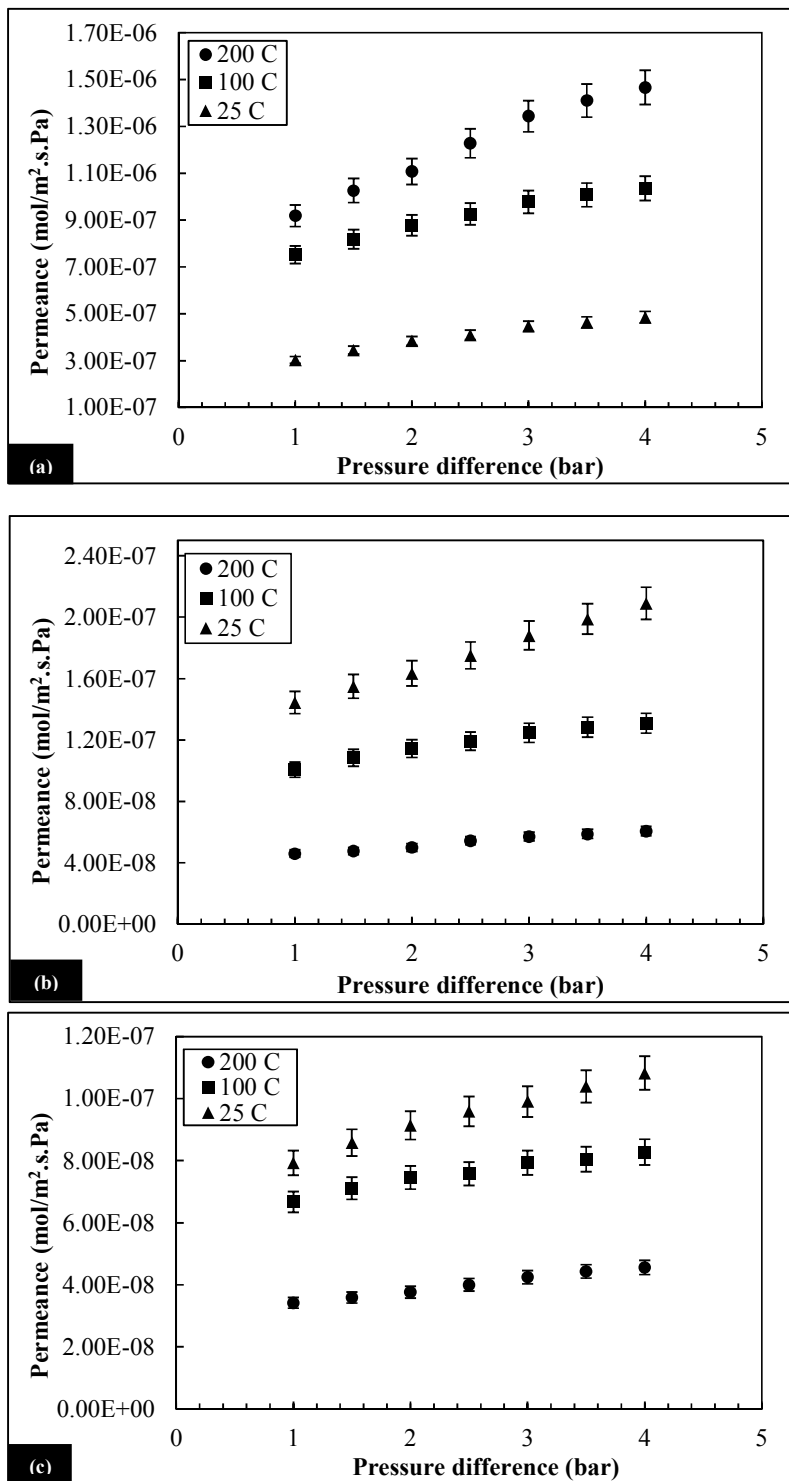


**Fig.6:** Pure gases permeance for synthesized silica membrane versus pressure difference at various temperatures: (a) H<sub>2</sub>, (b) CO<sub>2</sub> and (c) Ar.

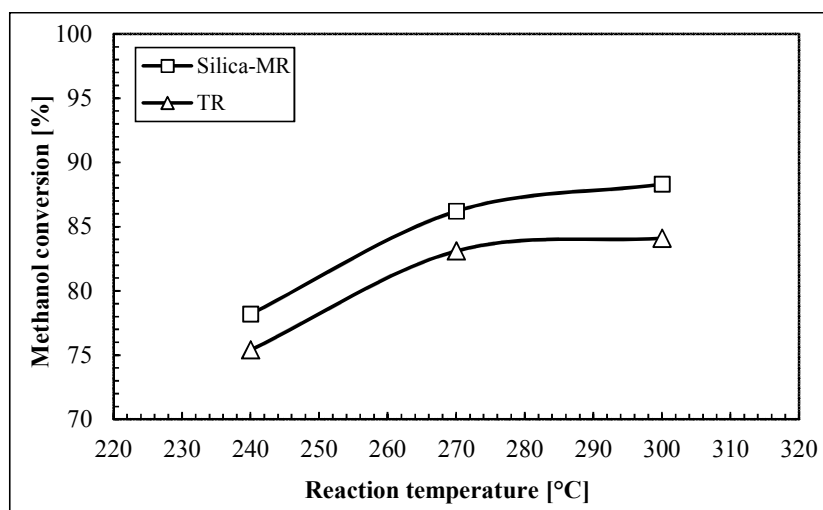


**Fig.7:** Methanol conversion versus reaction temperature for the silica MR and TR (at 1.5 bar,  $H_2O/CH_3OH=3$ ,  $Ar_{flow\ rate}=25\text{ ml/min}$  and  $GHSV=6000\text{ h}^{-1}$ ).

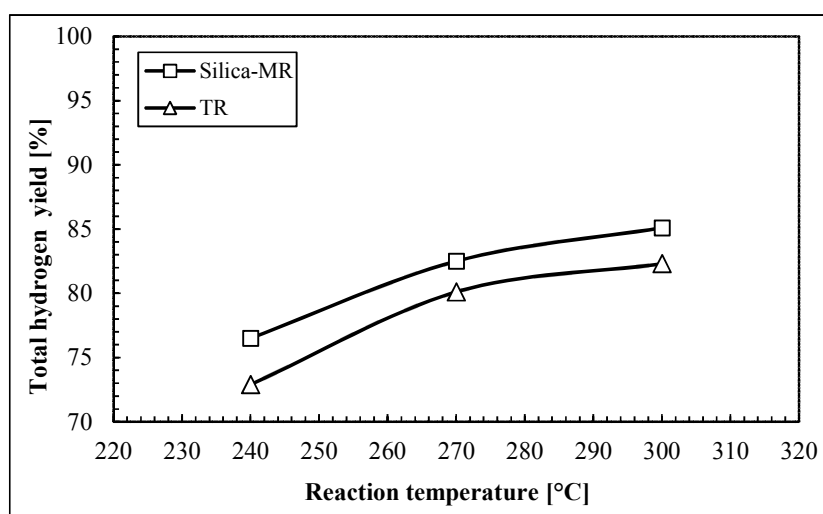


**Fig.8:** Total hydrogen yield versus reaction temperature for the silica MR and TR (at 1.5 bar,  $H_2O/CH_3OH=3$ ,  $Ar_{-flow\ rate}=25\text{ ml/min}$  and  $GHSV=6000\text{ h}^{-1}$ ).

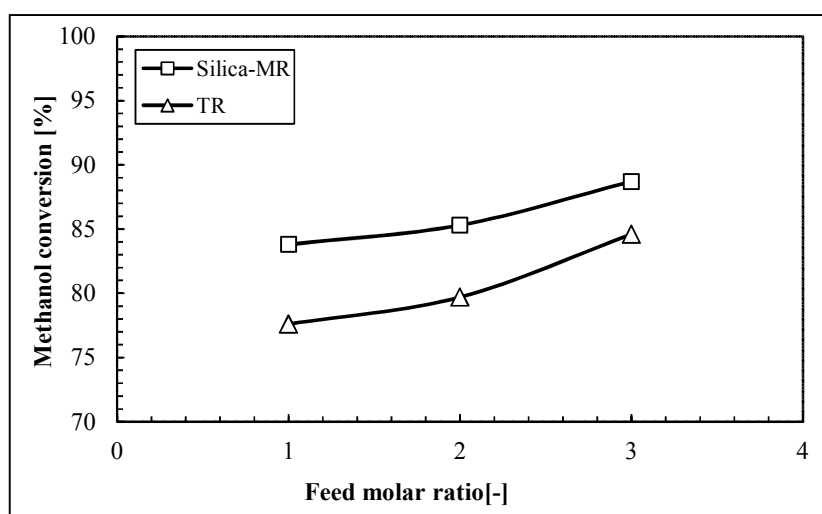


**Fig.9:** Methanol conversion versus feed molar ratio (steam/MeOH) for the silica MR and TR (at 1.5 bar, 300 °C,  $Ar_{\text{flow rate}} = 25 \text{ ml/min}$  and  $GHSV = 6000 \text{ h}^{-1}$ ).

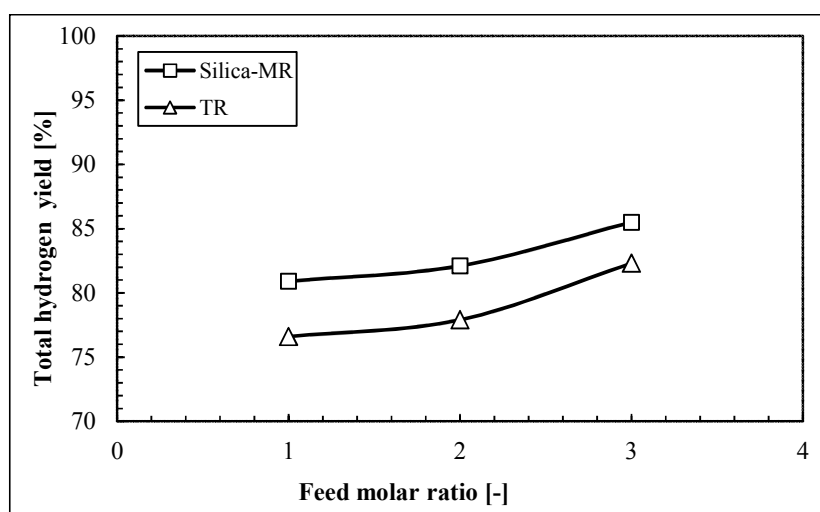


**Fig.10:** Total hydrogen yield versus feed molar ratio (Steam/MeOH) for the silica MR and TR (at 1.5 bar, 300 °C,  $Ar_{\text{-flow rate}}=25$  ml/min and  $GHSV=6000$  h<sup>-1</sup>).

**Tables:**

**Table 1.** The conditions of boehmite sol preparation and its particle size distribution for different layers.

The intermediate layer or coating sol	Molar ratio of Nitric Acid/Alkoxide	Aging time (min)	Particle size distribution (nm)
Boehmite sol of layer 1	0.026	1440	500-600
Boehmite sol of layer 2	0.026	5	200-300
Boehmite sol of layer 3	0.053	5	100-200
Boehmite sol of layer 4	0.070	5	40-100

**Table 2.** H<sub>2</sub>/CO<sub>2</sub>, H<sub>2</sub>/N<sub>2</sub> and H<sub>2</sub>/Ar permselectivity for synthesized silica membrane at different temperatures ( $\Delta p=2\text{bar}$ ).

Temperature	25 °C	100 °C	200 °C
H <sub>2</sub> /CO <sub>2</sub>	2.35	7.68	22.13
H <sub>2</sub> /N <sub>2</sub>	3.76	10.41	26.18
H <sub>2</sub> /Ar	4.21	11.76	29.42

**Table 3.** Comparing performance of synthesized silica membrane in this work with literatures data.

Membrane	H <sub>2</sub> /CO <sub>2</sub>	H <sub>2</sub> /N <sub>2</sub>	H <sub>2</sub> /Ar	Permeance H <sub>2</sub> (mol.m <sup>-2</sup> .s <sup>-1</sup> .Pa <sup>-1</sup> )	T(°C)	Pressure gradient (bar)	Ref
Silica	3.9	-	-	11.6×10 <sup>-7</sup>	100	1	[32]
Silica	6.8	-	-	17.4×10 <sup>-7</sup>	200	1	[32]
Silica	15.5	-	-	20.9×10 <sup>-7</sup>	400	0.2-1	[34]
Silica	41	-	-	4.04×10 <sup>-7</sup>	200	2	[32]
Silica	8	-	-	1.85×10 <sup>-7</sup>	200	1	[32]
Silica	-	32	-	10.7×10 <sup>-7</sup>	500	-	[35]
Silica	-	17	-	0.57×10 <sup>-7</sup>	220	-	[36]
Silica	-	8	-	20×10 <sup>-7</sup>	250	-	[32]
Silica	19.9	23.8	26.9	9.5×10 <sup>-7</sup>	200	1	This work
Silica	22.2	26.2	29.5	11.7×10 <sup>-7</sup>	200	2	This work

**Table 4.** The investigated conditions for the silica MR and TR.

Operating Parameters	Feed molar ratio (Steam/MeOH) Effect	Temperature Effect	GHSV Effect
Pressure (bar)	1.5	1.5	1.5
GHSV (h <sup>-1</sup> )	6000	6000	<b>6000-10000</b>
Temperature (°C)	300	<b>240-300</b>	300
H <sub>2</sub> O/CH <sub>3</sub> OH (-)	<b>1-3</b>	3	3

**Table 5.** CO selectivity and hydrogen recovery for silica MR and TR versus reaction temperature (at feed molar ratio 3, 1.5 bar,  $Ar_{\text{flow rate}} = 25 \text{ ml/min}$  and  $GHSV = 6000 \text{ h}^{-1}$ ).

Temperature (°C)	CO-Selectivity [%]		Hydrogen- Recovery [%]
	Silica-MR	TR	Silica-MR
240	0.49	0.68	30.83
270	1.35	1.72	34.71
300	1.61	2.01	37.95

**Table 6.** CO selectivity and hydrogen recovery for silica MR and TR versus feed molar ratio (at 300 °C, 1.5 bar, Ar<sub>flow rate</sub>= 25 ml/min and GHSV=6000 h<sup>-1</sup>).

Feed Molar Ratio	CO-Selectivity [%]		Hydrogen- Recovery [%]
	Silica-MR	TR	Silica-MR
1	3.3	5	43.1
2	2.49	3.21	41.3
3	1.61	2.01	37.95

**Table 7.** Methanol conversion and total hydrogen yield for silica MR and TR versus GHSV  
(at 300 °C, 1.5 bar, Ar-flow rate= 25 ml/min and feed molar ratio 3).

GHSV [h <sup>-1</sup> ]	Conversion [%]		Total yield [%]	
	Silica-MR	TR	Silica-MR	TR
6000	88.50	84.1	85.1	82.3
10000	82.61	79.10	79.62	76.8

**Table 8.** The CO selectivity and hydrogen recovery for silica MR and TR versus GHSV  
(at 300 °C, 1.5 bar, Ar-flow rate= 25 ml/min and feed molar ratio 3).

GHSV [h <sup>-1</sup> ]	CO-Selectivity [%]		Hydrogen- Recovery [%]
	Silica-MR	TR	Silica-MR
6000	1.61	2.01	37.9
10000	1.91	2.41	27.8